摩擦学学报
TRIBOLOGY

钛合金表面DLC薄膜的制备及其与不同材料配副的摩擦学性能研究

孙建芳，唐邕涛，苏峰华，李助军

Synthesis of DLC Film on Titanium Alloy and Its Tribological Property Sliding against Different Mating Materials

SUN Jianfang, TANG Yongtao, SU Fenghua, LI Zhujun

在线阅读 View online: https://doi.org/10.16078/j.tribology.2020231

DOI: 10.16078/j.tribology.2020231

钛合金表面DLC薄膜的制备及其与不同材料配副的摩擦学性能研究

孙建芳[1,2], 唐邕涛[1], 苏峰华[1*], 李助军[3]
(1. 华南理工大学 机械与汽车工程学院, 广东 广州 510641;
2. 清华大学 摩擦学国家重点实验室, 北京 100084;
3. 广州铁路职业技术学院 机械与电子学院, 广东 广州 510430)

摘 要: 利用等离子体增强化学气相沉积法(PECVD)在钛合金TC4表面制备了梯度结构DLC薄膜, 并研究了DLC薄膜微观形貌结构、力学性能以及不同对偶球材料(包括4种陶瓷与4种金属材料)对其摩擦学性能的影响. 结果表明: 所制备的梯度结构DLC薄膜表面相对光滑平坦且与基底结合紧密, 具有良好的力学性能; 对于陶瓷球/DLC配副, 在摩擦过程中由于对偶球硬度较大且耐磨, 从而在陶瓷球表面易于形成稳定的碳质转移膜, SiC/DLC、Si_3N_4/DLC和ZrO_2/DLC表现为轻微的磨粒磨损和黏着磨损, 而Al_2O_3球表面的碳元素含量较高使得DLC薄膜虽然发生破损和剥落但其摩擦系数仍保持在较低水平; 金属球/DLC与陶瓷/DLC相比较, 由于金属对偶球硬度较低, 在摩擦过程中碳质转移膜无法稳定地覆盖在金属球, 引起较高的摩擦系数, Al/DLC主要表现为严重的磨粒磨损, 而Brass/DLC、304SS/DLC和GCr15/DLC主要为轻微的磨粒磨损或黏着磨损; SiC/DLC、ZrO_2/DLC、304SS/DLC和GCr15/DLC的DLC薄膜均具有较低的摩擦系数和磨损率且对偶球的磨斑较小, 故其为较合理的摩擦副. 赫兹接触分析表明, 陶瓷/DLC中除了ZrO_2/DLC, 平均摩擦系数和计算接触半径的变化趋势是一致的, 而在金属/DLC中并未发现这一规律.

关键词: 钛合金; DLC薄膜; 对偶球; 摩擦磨损; 赫兹接触分析
中图分类号: TH117.3 **文献标志码:** A **文章编号:** 1004-0595(2021)06–0953–11

Synthesis of DLC Film on Titanium Alloy and Its Tribological Property Sliding against Different Mating Materials

SUN Jianfang[1,2], TANG Yongtao[1], SU Fenghua[1*], LI Zhujun[3]

(*1. School of Mechanical and Automotive Engineering, South China University of Technology, Guangdong Guangzhou 510641, China*
2. State Key Laboratory of Tribology, Tsinghua University, Beijing 100084, China
3. School of Mechanical and Electrical Engineering, Guangzhou Railway Polytechnic, Guangdong Guangzhou 510430, China)

Abstract: Diamond-like carbon (DLC) film with high hardness and excellent tribological properties, could improve the tribological performance of titanium alloy. At present, the tribological behavior of DLC film deposited on titanium alloy surface by the plasma enhanced chemical vapor deposition (PECVD) method, sliding against a variety of different ceramic and metal materials in air is worth studying. The graded DLC film was deposited on surface of a TC4 titanium

Received 27 October 2020, revised 3 February 2021, accepted 4 February 2021, available online 28 November 2021.
*Corresponding author. E-mail: fhsu@scut.edu.cn, Tel: +86-20-82313996.
The project was supported by the National Natural Science Foundation of China (51775191), the Tribology Science Fund of State Key Laboratory of Tribology of Tsinghua University (SKLTKF19B13) and Guangzhou Basic and Applied Basic Research Foundation (202102080422).
国家自然科学基金项目(51775191), 清华大学摩擦学国家重点实验室开放基金项目(SKLTKF19B13)和广州市基础与应用基础研究项目(202102080422)资助.

alloy by PECVD method. The microstructure, mechanical properties and the effect on the tribological properties for the as-prepared DLC films sliding against different mating ceramic balls and metal balls were investigated. The chemical composition and microstructure of the as-prepared DLC film were analyzed by Raman spectrum, scanning electron microscopy, energy dispersive spectrometer. The hardness and elastic modulus of the film were tested by nanoindentation. The bonding strength between the film and the substrate was measured by a scratch tester. The dry tribological performances of DLC film sliding against different ceramic and metal balls under air conditions were evaluated using a ball-on-disc wear tester. The results showed that the surface morphology of the graded DLC film was relatively smooth and uniform, and the film was well adhered to the substrate. The mechanical properties of deposited DLC film were excellent in this work. Eight tribo-pairs exhibited different friction and wear behaviors, and the ceramic/DLC pairs showed lower coefficient of friction and slighter wear of mating balls than the metal/DLC pairs, which were related to the properties of mating materials and action mechanism between the mating material and the DLC films. The possible friction and wear mechanisms of each tribo-pairs were further discussed. It suggested that for the ceramics/DLC tribo-pairs, it was easy to form stable carbonaceous transfer film on the ceramic balls due to high hardness and good wear resistance of the ceramic balls. SiC/DLC, Si_3N_4/DLC and ZrO_2/DLC exhibited mainly mild abrasive and adhesive wear while Al_2O_3/DLC revealed being damaged and peeled off but the friction coefficient was still at lower level because of the higher carbon content on the surface of the Al_2O_3 ball. And comparing the metals/DLC tribo-pairs with the ceramics/DLC tribo-pairs, it was difficult to maintain stable carbonaceous transfer film on the metal balls due to lower hardness of the metal balls, resulting in higher friction coefficient. Al/DLC exhibited mainly severe abrasive wear while brass/DLC, 304SS/DLC and GCr15/DLC revealed mild abrasive or adhesive wear. It also suggested that SiC/DLC, ZrO_2/DLC, 304SS /DLC and GCr15/DLC can be reasonable tribo-pairs because of relatively lower friction coefficients and wear rates of the DLC films and the small wear scars. Hertzian contact analysis showed that the variation trend of average friction coefficient and calculated contact radius was consistent in the ceramic/DLC tribo-pairs except ZrO_2/DLC, but this phenomenon was not found in metals /DLC tribo-pairs.

Key words: titanium alloy; DLC film; mating balls; friction and wear; Hertzian contact analysis

钛合金具有强度高、密度低、耐腐蚀和良好的抗疲劳性能等优点，广泛应用于机械、航空和生物医学等各个领域，但其较差的摩擦学性能阻碍了其在苛刻工况条件下的应用[1-3]，通常采用涂层、热氧化和化学热处理等表面处理方法改善其力学性能和摩擦学性能[4-6]，其中真空镀膜作为涂层中一种有效的表面改性方法，通过在超高真空下对基材表面进行功能薄膜的沉积从而改善基材表面性能和摩擦学性能.

类金刚石薄膜(DLC)是1种典型的真空镀膜，具有高硬度、优异的摩擦学性能、良好的化学惰性和生物相容性等优点[7-9]. DLC薄膜的摩擦学性能受基底材料、制备工艺和使用条件等因素的影响，在实际应用中与不同对偶材料组成摩擦副时也受到对偶材料的影响[10-15]. 王等[16]发现配副材料对钢基材上氟化DLC薄膜的摩擦学行为有不同的影响机制；Li等[17]研究发现DLC薄膜在潮湿的N_2中与Si_3N_4、Al_2O_3和钢球配副的摩擦磨损行为取决于摩擦诱导化学作用；郑等[18]以第一性原理研究了真空和CO_2环境对于DLC与Al和ZrO_2配副摩擦性能的影响，发现不同环境中对偶球与薄膜形成不同的化学键是影响摩擦性能的关键；Cui等[19]研究了含氢DLC薄膜与不同陶瓷球配副的真空摩擦学行为，结果表明对偶材料与碳之间的附着力对DLC薄膜的真空摩擦学行为有较大影响；Wu等[20]研究了304不锈钢基材上制备的DLC薄膜在空气和氢气里与不同陶瓷对偶材料干摩擦时的摩擦学性能，发现其摩擦学性能受气体环境和对偶配副材料的影响，在空气中WC球和ZrO_2球摩擦副分别具有最低的摩擦系数和磨损率.

以往研究对偶材料对DLC薄膜摩擦学性能的影响中，采用的基材、制备工艺和试验环境各不相同，然而不同的基材和制备工艺对薄膜的结构、承载能力和结合力方面的影响不同，从而与相同的材料配副的摩擦磨损性能也不同. 等离子体增强化学气相沉积法(PECVD)是一种真空镀膜方法，具有工艺简单、沉积温度低和成膜质量好等优点，可以在常温下制备出光滑致密的DLC薄膜. 目前钛合金上制备DLC薄膜已有大量研究，但利用PECVD工艺在钛合金上制备梯度DLC薄膜并用于探索多种金属对偶球和陶瓷对偶球对其摩擦学性能影响的研究还尚未发现. 基于此，本文作者在钛合金基材上制备梯度DLC薄膜并研究其在常温空气中与4种陶瓷球和4种金属球配副的干摩擦磨损行为，并对其摩擦磨损机理进行分析，为DLC薄膜实际应用提供依据.

1　试验部分

1.1　DLC薄膜的制备

基材选用尺寸为40 mm×20 mm×5 mm的TC4钛合金，先依次使用400、800、1 200、1 500和2 000目砂纸打磨后，抛光至表面粗糙度小于40 nm，最后用无水乙醇超声波清洗，吹干备用. 然后，使用PVD/PECVD复合离子镀膜设备镀制DLC薄膜. 先将真空度抽至低于1×10^{-3} Pa，随后通入氩气并开启霍尔离子源及偏压电源，在0.3 Pa真空度下产生等离子体对基材轰击清洗以去除其表面的杂质. 最后，为了提高基材与DLC薄膜的结合力，采用中频双靶磁控溅射在基材和DLC薄膜之间制备Ti/TiN/TiCN过渡层，采用等离子体增强化学气相沉积法制备DLC薄膜. 制备Ti/TiN/TiCN/DLC的具体工艺参数列于表1中, 其中气体流量单位为标准毫升/分钟(sccm).

1.2　DLC薄膜的微观结构和摩擦学性能测试

采用LabRAM Aramis拉曼光谱仪获取薄膜的拉曼光谱；采用NOVA NANOSEM 430扫描电子显微镜(SEM)观察DLC薄膜的表面和断面形貌；采用扫描电镜配带的能谱仪(EDS)分析DLC膜的断面元素组成；采用Agilent Technologies Nano Indenter 200纳米压痕仪测试DLC膜的硬度和弹性模量，测试深度为1 mm；采用划痕测试仪测试薄膜的结合力，加载速率为60 N/min，长度约为5 mm；采用Talysurf CLI 1 000表面轮廓仪测量基材和DLC薄膜的表面粗糙度.

采用UMT TriboLab型多功能摩擦磨损试验机，以球-盘摩擦方式进行旋转摩擦试验. 分别选取工程应用中常见的4种陶瓷球(Al_2O_3、SiC、Si_3N_4、ZrO_2)和4种金属球(304 SS、GCr15、Al、Brass)作为对偶球，直径为6 mm，其机械性能列于表2中，硬度和弹性模量相对于薄膜从小到大均有分布. 摩擦试验条件如下：载荷为10 N，干摩擦转速为200 r/min，旋转半径为5 mm，时间为3 600 s. 试验过程由计算机自动记录试验数据，每组试验进行3次重复. 摩擦试验后，采用SEM观察DLC薄膜和对偶球的磨痕；采用EDS分析对偶球磨斑的元素成分；采用Talysurf CLI 1 000表面轮廓仪测量DLC薄膜的磨损宽度和深度，计算平均磨损体积，求出磨损率. 磨损率由公式$K=V/(S\cdot F)$计算得到，其中V为磨损体积(单位mm^3)，S为总滑动距离(单位m)，F为法向载荷(单位N).

表 1　制备Ti/TiN/TiCN/DLC薄膜及过渡层的工艺参数

Table 1　Deposition parameters of Ti/TiN/TiCN/DLC film production

Layers	Ar/sccm	N_2/sccm	C_2H_2/sccm	H_2/sccm	Time/min	Pulse voltage/V	DC voltage /V	Current /A	Duty ratio /%
Substrate	50	0	0	0	30	−600	−100	−	40
Ti	25	0	0	0	10	−300	−80	−2.5	20
TiN	30	15	0	0	15	−200	−60	2.5	15
TiCN	45	40	40	0	30	−200	−60	2.5	15
DLC	0	0	80	20	120	−1 600	−	−	15

表 2　对偶球的机械性能

Table 2　Mechanical properties of mating balls

Materials	Hardness/GPa	Elastic modulus/GPa	Poisson's ratio
Al_2O_3	16.2	210	0.3
SiC	27.4	440	0.17
Si_3N_4	14.7	320	0.26
ZrO_2	11.8	340	0.22
304 SS	2.2	194	0.3
GCr15	6.9	208	0.3
Al	<0.2	71	0.31
Brass	<1	93	0.34

2　结果与讨论

2.1　DLC薄膜的微观结构和机械性能

图1给出了DLC薄膜的拉曼光谱、表面和断面形貌以及断面线扫描成分. 如图1(a)所示，所制备的薄膜在1 500 cm^{-1}左右有1个不对称的宽峰，利用高斯函数分峰后，在1 347和1 538 cm^{-1}位置分别对应D峰和G峰，这是典型的DLC薄膜的拉曼光谱特征[21]. D峰和G峰的积分面积比I_D/I_G能够间接反应DLC薄膜中sp^3杂化键和sp^2杂化键的相对含量比，I_D/I_G越大意味着DLC薄膜具有更高的石墨化程度[8,22]，所制备薄膜拉曼光谱的I_D/I_G为0.81.

由图1(b)可知，薄膜均匀致密，与基体之间没有明显的分层和缺陷，膜厚约为4.7 μm. 由图1(c)可知，薄膜表面相对光滑平坦，有少量团聚的颗粒可见，表面粗糙度约为28 nm，略小于钛合金基材，说明所选择的脉冲偏压数值合适，并未增加薄膜表面粗糙度. 由图1(d)可知，薄膜断面主要包括过渡层的Ti、N元素和C元素

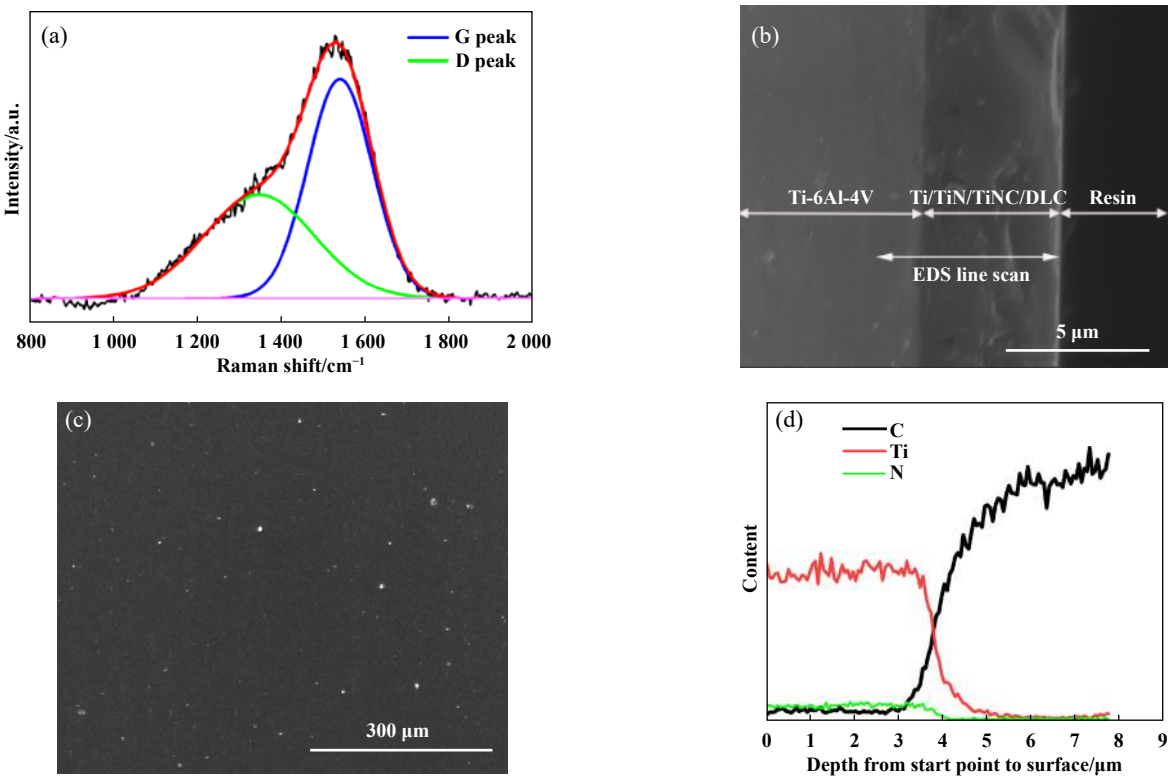

Fig. 1 (a) Raman spectrum, (b) SEM micrograph of cross-section and (c) surface, (d) section line scans the component of Ti/TiN/TiNC/DLC film

图 1 Ti/TiN/TiNC/DLC薄膜的(a)拉曼光谱, (b)断面和(c)表面形貌以及(d)断面线扫描成分

及最外层的C元素, 薄膜为梯度过渡的Ti/TiN/TiNC/DLC的复合薄膜, Ti/TiN/TiNC过渡层较薄, DLC膜层较厚且为主要的功能层. 划痕试验测得薄膜的膜基结合力约为34 N, 说明引入复合过渡层能够缓解薄膜内应力且可防止DLC薄膜脱落[23-24]; 纳米压痕测得薄膜的弹性模量和硬度分别为117 GPa和14.4 GPa, 说明所制备的薄膜具有较好的力学性能.

2.2 DLC薄膜与不同陶瓷球的摩擦磨损性能分析

图2给出了DLC薄膜与4种陶瓷球进行干摩擦的实时摩擦曲线、平均摩擦系数和磨损率对比数据图. 由图2(a)可知, 摩擦过程分为初始摩擦阶段和稳定摩擦阶段, Al_2O_3/DLC和ZrO_2/DLC摩擦副的摩擦系数曲线变化相对稳定, 而SiC/DLC与Si_3N_4/DLC摩擦副的摩擦系数曲线波动较大. 图2(b)给出了平均摩擦系数和DLC薄膜的磨损率对比数据, 在稳定摩擦阶段, Al_2O_3/DLC、SiC/DLC、Si_3N_4/DLC和ZrO_2/DLC的平均摩擦系数分别为0.110、0.094、0.096和0.077, 对应的DLC磨损率分别为1.632×10^{-6}、0.498×10^{-6}、0.669×10^{-6}和$0.245\times$

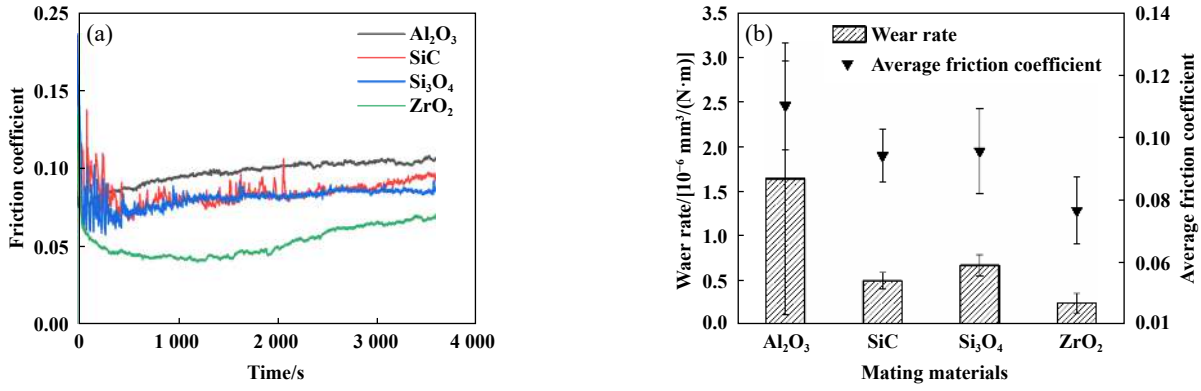

Fig. 2 (a) Real-time friction coefficient, (b) average friction coefficients and wear rates for different ceramics/DLC film tribo-pairs

图 2 陶瓷球/DLC摩擦副的(a)实时摩擦系数曲线和(b)平均摩擦系数和磨损率

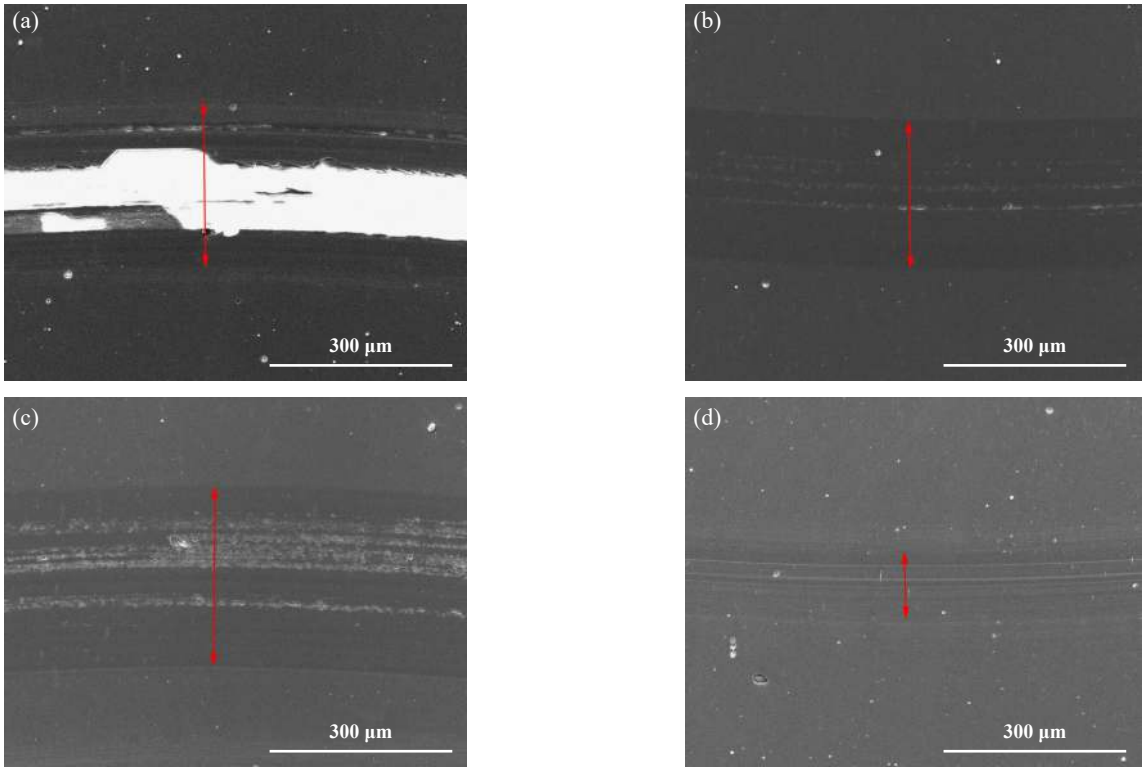

Fig. 3 SEM micrographs of wear tracks of DLC films sliding against different ceramic balls: (a) Al_2O_3/DLC; (b) SiC/DLC; (c) Si_3N_4/DLC; (d) ZrO_2/DLC

图 3　与不同陶瓷球摩擦的DLC薄膜磨痕扫描电镜照片: (a)Al_2O_3/DLC; (b)SiC/DLC; (c)Si_3N_4/DLC; (d)ZrO_2/DLC

表 3　与陶瓷球摩擦后的DLC磨痕表面典型元素的相对原子分数(%)

Table 3　Relative atomic fractions of the wear tracks of DLC films after sliding against ceramic balls (%)

Wear tracks of DLC films	Relative atomic fraction/%						
	C	O	Al	Si	Zr	Ti	Others
Al_2O_3/DLC	37.03	5.75	2.26	–	–	51.21	3.75
SiC/DLC	79.05	18.37	–	2.28	–	0.29	0.01
Si_3N_4/DLC	64.55	22.62	–	10.18	–	0.46	2.19
ZrO_2/DLC	83.59	12.16	–	–	3.77	0.48	0

10^{-6} $mm^3/(N·m)$.

图3给出了与不同陶瓷球摩擦后DLC表面磨损形貌的SEM照片，表3给出了通过EDS测试的DLC磨痕表面磨屑的元素. 由图3可知，不同对偶球对薄膜磨痕形貌有不同影响. 球-盘干摩擦60 min后，与Al_2O_3摩擦的DLC磨损最严重，磨痕宽度和深度分别约为300 μm和4 μm，薄膜发生较严重的破损和剥落，低摩擦系数说明并未摩擦至钛合金基底，表面较高的Ti元素含量说明DLC严重磨损且磨痕已至过渡层. 与Si_3N_4和SiC摩擦的DLC磨痕表面出现明显的犁沟和黏着斑坑，前者磨损程度较高，两种摩擦副的磨损机理为轻微的磨粒磨损和黏着磨损. 与ZrO_2摩擦的DLC磨痕最窄，宽度约150 μm，深度约0.1 μm，磨痕整体光滑，仅有少量浅沟，磨损机理为轻微的磨粒磨损. 4种不同陶瓷球摩擦后DLC薄膜的磨痕均检测出少量对偶球的元素成分，说明对偶材料有一部分向薄膜转移，磨痕中氧元素表明薄膜经过摩擦发生了轻微氧化. 梯度的TiN/TiCN缓冲了薄膜沉积产生的应力，强化膜层交互，增强了其承载能力，导致薄膜耐磨性强，磨损量低.

图4给出了与DLC薄膜摩擦后不同陶瓷球磨斑形貌的SEM照片. 从图4(a~d)可知，陶瓷球磨损轻微，表面划痕较少，有轻微的脆性剥落，Al_2O_3、Si_3N_4、SiC和ZrO_2对偶球的磨损范围直径分别约为300、280、250和150 μm. 通过EDS分别测试图4中陶瓷球磨斑P1、P2、P3和P4区域的化学元素，典型元素的相对原子分数值列于表4中. 由表4可知，所有陶瓷球的磨斑上都发现

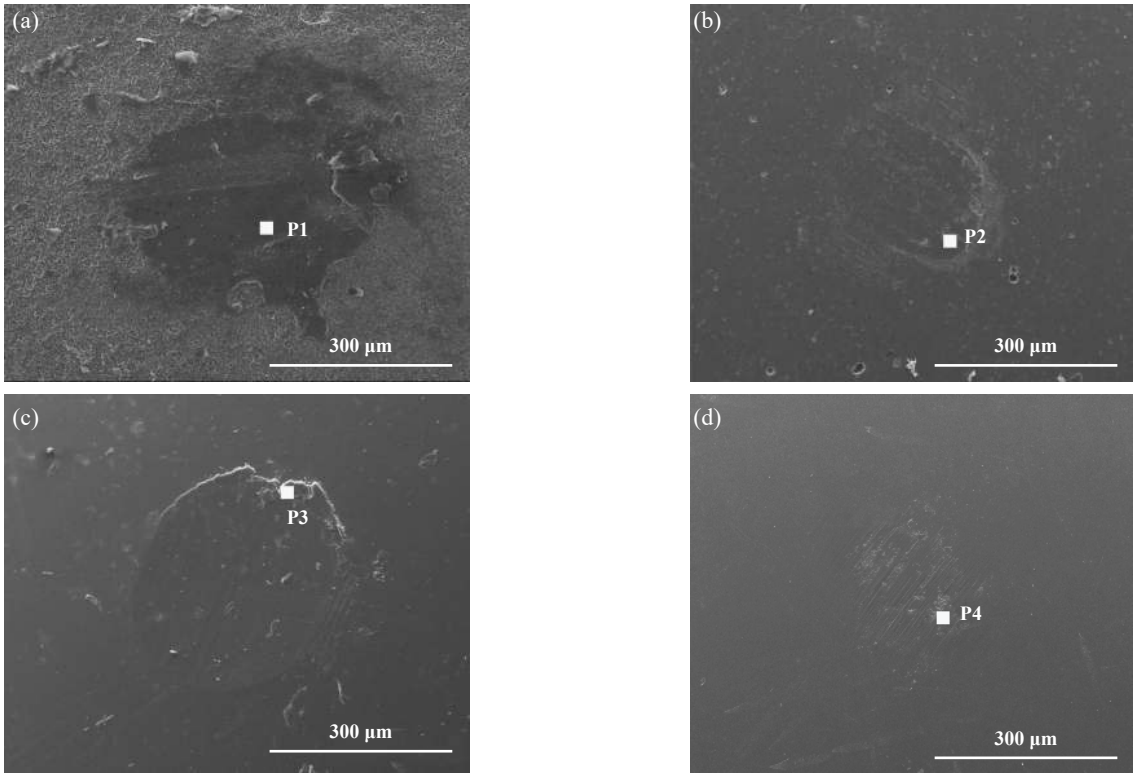

Fig. 4 SEM micrographs of wear scars of different ceramic balls after sliding against DLC film: (a) Al_2O_3; (b) SiC; (c) Si_3N_4; (d) ZrO_2

图 4 与DLC摩擦后不同陶瓷球磨斑的扫描电镜图: (a) Al_2O_3, (b) SiC; (c) Si_3N_4, (d) ZrO_2

表 4 与DLC摩擦后陶瓷球磨斑表面典型元素的相对原子分数

Table 4 Relative atomic fractions of the wear scars of ceramic balls after sliding against DLC films

Wear scars of ceramic balls	Relative atomic fraction/%				
	C	O	Al	Si	Zr
Al_2O_3	80.53	8.69	10.48	–	–
SiC	38.48	40.23	–	21.28	–
Si_3N_4	33.75	42.51	–	23.75	–
ZrO_2	26.34	49.26	–	–	24.4

了碳元素，说明陶瓷球上存在DLC薄膜的碳质转移膜. 其中Al_2O_3对偶球上C原子分数达80.5%，一方面较高硬度的Al_2O_3球对薄膜造成较强的磨削作用，另一方面Al_2O_3是一种弱Lewis酸，可以被用作碳氢化合物的催化剂，在空气中摩擦作用下，Al_2O_3球可能对DLC薄膜进行催化降解，导致DLC的C-H键断裂，薄膜失效，宏观上表现为薄膜磨损率大[17]. 磨损产生大量的碳质磨屑填充在磨痕里并随摩擦逐渐转移到球表面形成较厚的转移膜，阻碍了对偶球与过渡层直接接触，降低了摩擦作用力从而阻止了薄膜被彻底磨穿，进一步说明了Al_2O_3/DLC虽然磨损严重，但摩擦系数可以保持在稳定低水平. 对于SiC和Si_3N_4两种对偶球，Si对碳有较强的亲和性，有利于碳质转移膜生成[16]，Si_3N_4可能在摩擦界面形成Si-C键，产生较强的黏着，导致摩擦系数波动大且磨痕磨损更明显. ZrO_2对偶球对碳的黏着倾向微弱，在摩擦界面形成弱的C-O键，易发生分离，导致最小的摩擦系数和最轻微的磨损形貌[18-19]. 另外，陶瓷球不易磨损，球面上形成相对稳定的碳质转移膜，减小了球和薄膜受到的摩擦剪切作用，所以陶瓷/DLC摩擦副表现出良好的摩擦学性能. 综合比较分析，由于SiC/DLC和ZrO_2/DLC中DLC薄膜摩擦系数和磨损率均较低，SiC和ZrO_2对偶球的磨斑也较小，因此SiC/DLC和ZrO_2/DLC是比较合适的摩擦副.

2.3 DLC薄膜与不同金属球的摩擦磨损性能分析

图5给出了DLC薄膜与4种金属球进行干摩擦的实时摩擦曲线、平均摩擦系数和磨损率对比数据图. 由图5(a)可知，Al/DLC和304SS/DL摩擦副的摩擦系数曲线变化相对稳定，而Brass/DLC和GCr15/DLC摩擦

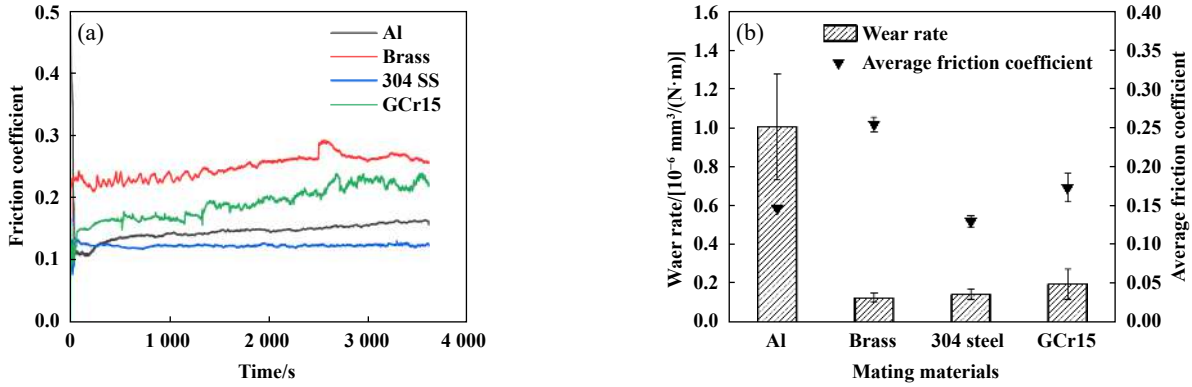

Fig. 5 (a) Real-time friction coefficient and (b) average friction coefficients and wear rates of different metals/DLC film tribo-pairs

图 5　金属球/DLC摩擦副的(a)实时摩擦系数曲线和(b)平均摩擦系数和磨损率

副的摩擦系数曲线波动较大. 图5(b)给出了平均摩擦系数和DLC薄膜的磨损率对比数据，在稳定摩擦阶段，Al/DLC、Brass/DLC、304 SS/DLC和GCr15/DLC的平均摩擦系数分别为0.148、0.256、0.131和0.174，对应的DLC磨损率分别为1.009×10^{-6}、0.132×10^{-6}、0.148×10^{-6}和0.202×10^{-6} mm^3/(N·m). 由图2和图5比较可知，金属球/DLC摩擦副的摩擦系数均大于陶瓷球/DLC摩擦副的摩擦系数，与金属球配副的DLC磨损率小于与陶瓷球配副的磨损率.

图6给出了与不同金属球摩擦后DLC表面磨损形貌的SEM照片，表5给出了通过EDS测试的DLC薄膜磨痕表面元素. 如图6所示, 与Al对偶球摩擦的DLC磨痕宽度和深度分别约为600 μm和0.3 μm，磨痕上的犁沟为边缘深而中心浅，其磨损机理为严重的磨粒磨损. 由表5可知，磨痕表面存在Al元素，较大的硬度差使铝球向较硬的薄膜发生材料转移，易被氧化的纯铝在摩擦作用下产生了硬质氧化物磨粒，一方面硬度大的氧化铝磨粒对DLC薄膜进行严重的微切削，另一方面可能对薄膜有一定催化降解效果，导致对应DLC薄膜磨损率最大，在摩擦过程中磨粒富集在磨痕边缘并对边

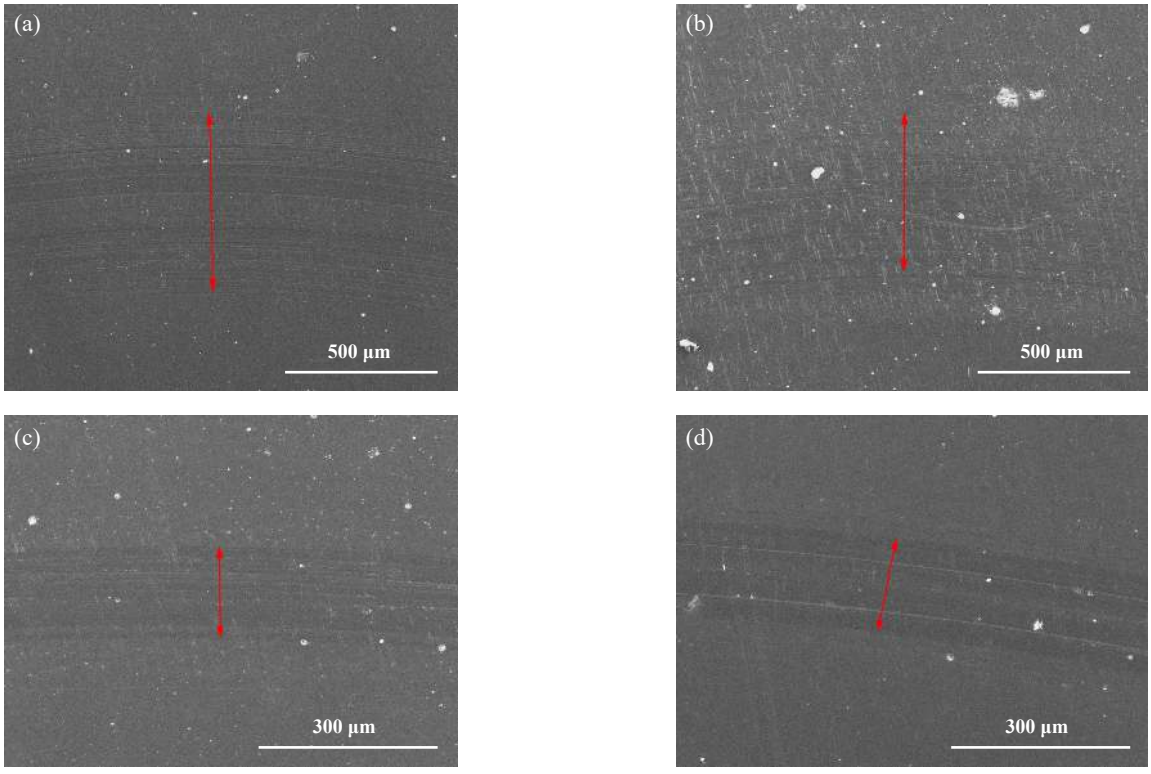

Fig. 6 SEM micrographs of wear tracks of DLC films sliding against different metal balls: (a) Al; (b) Brass; (c) 304SS; (d) GCr15

图 6　与不同金属球摩擦的DLC薄膜磨痕形貌扫描电镜照片：(a) Al；(b) Brass；(c) 304 SS；(d) GCr15

表 5 与金属球摩擦后的DLC薄膜磨痕表面典型元素的相对原子分数

Table 5 Relative atomic fractions of the wear tracks of DLC films after sliding against metal balls

Wear tracks of DLC films	Relative atomic fraction/%						
	C	O	Al	Fe	Cu	Zn	Others
Al/DLC	42.36	44.54	12.87	–	–	–	0.23
Brass/DLC	30.06	10.59	–	–	36.45	21.68	1.22
304 SS/DLC	83.74	11.64	–	3.09	–	–	1.53
GCr15/DLC	71.32	13.72	–	13.21	–	–	1.25

缘区域产生剧烈作用；另外，大量硬质磨粒使滑动摩擦变为滚动摩擦，因此Al/DLC的摩擦系数并不高. 与Brass对偶球摩擦的DLC磨痕宽度和深度分别为600 μm和0.05 μm，磨损极其轻微，磨痕处有少量极浅的沟槽和细小的黏着斑点，其磨损机理为轻微的黏着磨损. 由表5可知，磨痕处Cu原子分数达36.45%，这是因为具有较高的塑性和黏着性的Brass易于向较硬的DLC薄膜大量转移，Brass球面严重的磨损增加了接触面的粗糙度，微凸体咬合提高了摩擦系数，但软质Brass球难以对硬的DLC薄膜造成可观的磨损量，从而该摩擦副摩擦系数最大但对应薄膜的磨损率最小. 与304SS对偶球和GCr15对偶球摩擦的DLC磨痕宽度和深度相近，分别约为150和0.1 μm，与后者摩擦的DLC磨痕处存在更多Fe元素，可能是在高速摩擦过程中GCr15比304SS更容易与空气中的氧气和水发生化学反应，生成一些铁的氧化物且与薄膜黏着，摩擦系数较高，而304 SS是以磨粒磨损为主，导致对应的DLC磨痕上有更多的浅犁沟，磨粒作为微小滚珠降低了摩擦系数；另外，GCr15的硬度高于304SS，导致对应的DLC薄膜更易被磨损.

图7给出了与DLC薄膜摩擦后不同金属球磨斑形貌的SEM照片. 由图7(a~d)可知，Al、Brass、304SS和GCr15对偶球的磨损范围直径分别约为900、800、300和300 μm. 由图4和图7比较可知，金属球磨斑明显大于陶瓷球，这是因为金属球硬度远低于陶瓷球和DLC薄膜，虽然摩擦过程中产生的碳质转移膜降低球面受到的剪切作用，但仍然不足以阻止金属球接触界面的剪切破坏，金属磨粒不断向摩擦界面转移并加剧

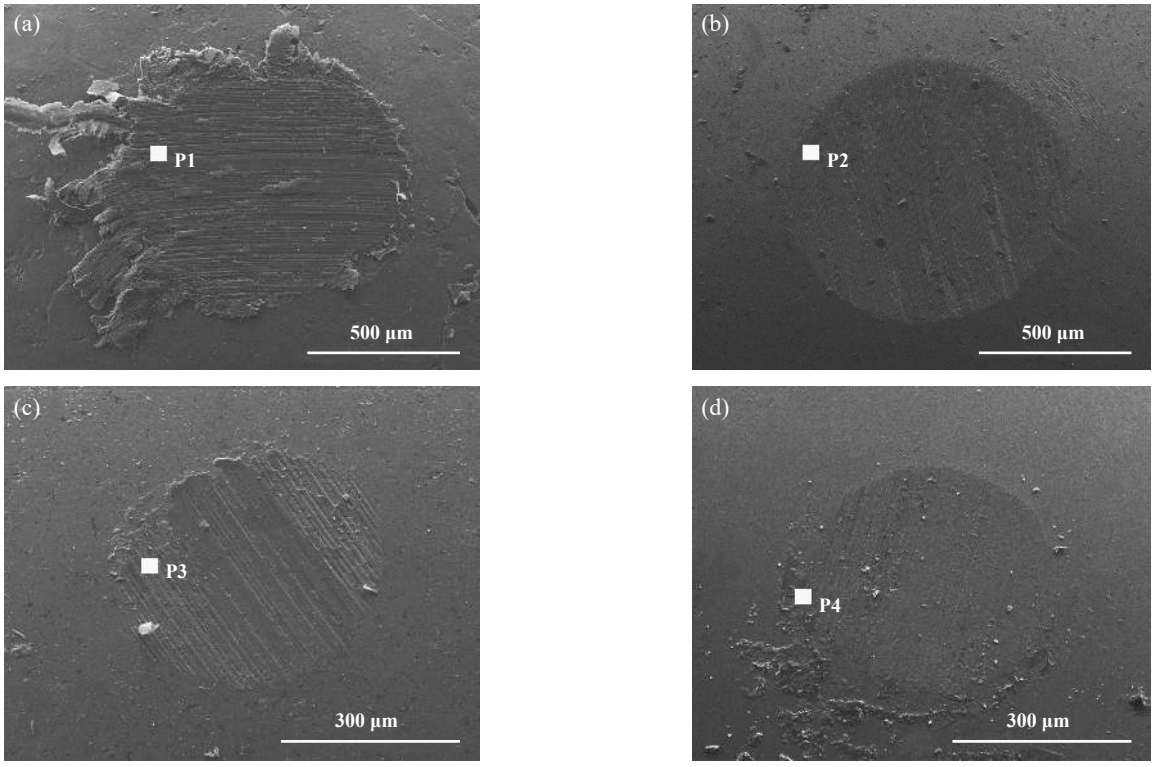

Fig. 7 SEM micrographs of wear scars of different metal balls after sliding against DLC film: (a) Al; (b) Brass; (c) 304 SS; (d) GCr15

图 7 与DLC摩擦后不同金属球磨斑形貌的扫描电镜照片：(a) Al；(b) Brass；(c) 304 SS；(d) GCr15

表 6　与DLC摩擦后的金属球磨斑表面典型元素的相对原子分数

Table 6　Relative atomic fractions of the wear scars of metal balls after sliding against DLC films

Wear scars of metal balls	Relative atomic fraction/%						
	C	O	Al	Fe	Cu	Zn	Others
Al	14.73	56.53	28.75	–	–	–	–
Brass	47.88	26.04	–	–	16.22	9.86	–
304SS	25.59	21.46	–	38.17	0.4	–	14.38
GCr15	23.84	13.10	–	60.36	–	–	2.7

了金属球的磨损，导致DLC薄膜的碳质转移膜不能稳定地保持在金属球表面，从而造成金属球自身磨损较大，减摩抗磨作用相对较差. 通过EDS分别测试图7中金属球磨斑P1、P2、P3和P4区域的化学元素，典型元素的相对原子分数如表6所示. 由表4和表6比较可知，所有金属球的磨斑上的碳元素含量都低于陶瓷球，进一步表明碳质转移膜随金属磨损而流失，所以陶瓷/DLC摩擦副比金属/DLC摩擦副表现出更好的摩擦学性能. 综合分析，由于304SS/DLC和GCr15/DLC中DLC薄膜具有相对较低的摩擦系数和磨损率以及对偶球的磨斑也较小，因此，304SS/DLC和GCr15/DLC是比较合适的摩擦副.

2.4　对偶球接触半径与摩擦系数的关系

赫兹接触半径与摩擦系数的关系通常可以用来分析DLC薄膜的摩擦学性能[25-26]. 因此引入了赫兹接触分析，接触半径可由式(1)计算.

$$a=\left(\frac{3FR}{4E'}\right)^{\frac{1}{3}} \tag{1}$$

式中：a为接触半径(mm)，F为法向载荷(N)，R为球的半径(mm)，E'为有效弹性模量(GPa)，E'可按式(2)计算.

$$\frac{1}{E'}=\frac{1-\upsilon_1^2}{E_1}+\frac{1-\upsilon_2^2}{E_2} \tag{2}$$

式中：E_1和E_2、υ_1和υ_2分别为DLC薄膜和对偶材料的弹性模量(单位GPa)、泊松比. 表7给出了计算得到的有效弹性模量和接触半径.

不同摩擦副的接触半径与摩擦系数的关系如图8所示. 图8(a)中，对于陶瓷/DLC摩擦副，摩擦系数的变化趋势与接触半径相似，表明摩擦系数与接触半径存在某种相关性. 摩擦系数和球面上碳质转移膜的形成有关，球-盘的接触面积随接触半径的减小而减小，较小的接触面积增加了转移膜的有效覆盖区域[27]. 由表7可知，ZrO_2/DLC和SiC/DLC的接触半径分别为0.061 9和0.060 7 mm，而ZrO_2/DLC的摩擦系数比SiC/DLC降

表 7　摩擦配副的有效弹性模量和接触半径

Table 7　Effective elastic modulus and Hertzian contact radius of the counterpart balls

Mating materials	Al_2O_3	SiC	Si_3N_4	ZrO_2	Al	Brass	304SS	GCr15
Effective elastic modulus/GPa	82.6	100.2	93.5	94.6	48.8	57.9	80.2	82.3
Contact radius/(10^{-2} mm)	6.48	6.07	6.22	6.19	7.72	7.29	6.55	6.49

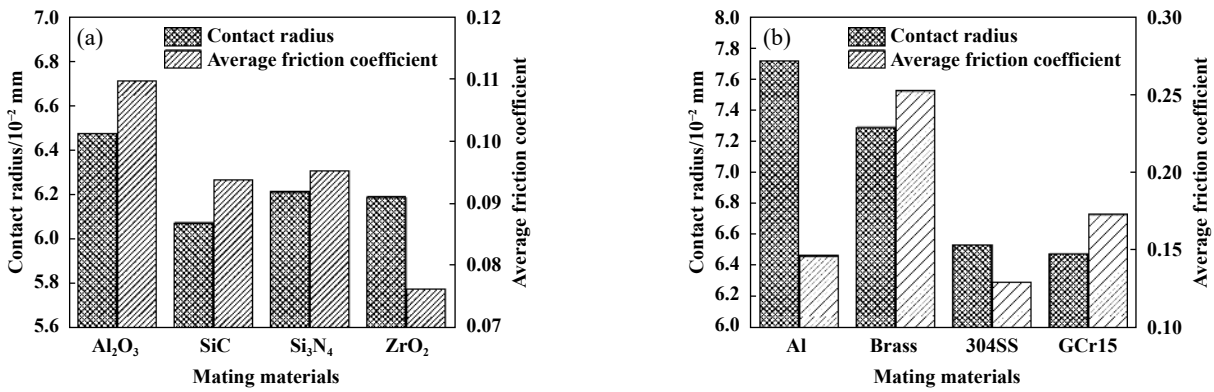

Fig. 8　Relationship between Hertzian contact radius and friction coefficients for DLC film with (a) ceramics and (b) metal mating balls

图 8　DLC薄膜与(a)陶瓷球及(b)金属球的赫兹接触半径与摩擦系数的关系

低了37.14%，这表明ZrO_2/DLC较小的接触面积增加了转移膜的有效覆盖区域，导致其摩擦系数最小，进一步解释了ZrO_2/ DLC干摩擦试验结果. 如图8(b)所示，对于不同的金属摩擦副，摩擦系数随接触半径变化没有发现明显的规律，这是由于一方面金属球的磨斑远大于陶瓷球的磨斑，摩擦过程中金属球的实际接触半径与公式计算得到的初始接触半径相差较大；另一方面金属球与DLC摩擦时受到材料特性及摩擦化学反应等其他复杂因素影响较明显，故其初始接触半径与摩擦系数没有明显的相关性.

3 结论

a. 利用PECVD方法在TC4钛合金基材上制备了Ti/TiN/TiNC/DLC的表面梯度复合薄膜，该复合薄膜与钛合金基底结合紧密且断面膜层较均匀，具有较好的力学性能.

b. 进行了DLC薄膜对不同陶瓷球干摩擦学性能研究，结果表明，在摩擦磨损过程中由于陶瓷球具有较高的硬度和耐磨性，陶瓷球上存在比较稳定的DLC薄膜的碳质转移膜. SiC/DLC、Si_3N_4/DLC和ZrO_2/DLC表现为轻微的磨粒磨损和黏着磨损，而Al_2O_3/DLC的薄膜发生破损和剥落. SiC/DLC和ZrO_2/DLC的摩擦系数和DLC磨损率均较低，SiC和ZrO_2对偶球的磨斑也较小，因此SiC/DLC和ZrO_2/DLC是较合适的摩擦副.

c. 进行了DLC薄膜对不同金属球干摩擦学性能研究，结果表明，在摩擦磨损过程中，与陶瓷/DLC摩擦副相比，低硬度的金属球易磨损，碳质转移膜随球磨损而流失，导致摩擦系数比陶瓷/DLC高. Al/DLC主要表现为严重的磨粒磨损，而Brass/DLC主要为轻微的黏着磨损，304SS/DLC和GCr15/DLC为轻微的磨粒磨损和黏着磨损. 304SS/DLC和GCr15/DLC具有较低的摩擦系数、DLC薄膜的低磨损率以及较小的球磨斑，因此304SS/DLC和GCr15/DLC也是较合适的摩擦副.

d. 根据赫兹接触分析计算各摩擦副的接触半径，结果表明，陶瓷/DLC的摩擦系数与初始接触半径的变化趋势相似，二者存在着一定的相关性；而对于金属/DLC的摩擦系数与初始接触半径没有明显的相关性.

参 考 文 献

[1] Ghahramanzadeh Asl H. Investigation of friction and wear performance on oxidized Ti6Al4V alloy at different temperatures by plasma oxidation method under ambient air and vacuum conditions[J]. Vacuum, 2020, 180: 109578. doi: 10.1016/j.vacuum.2020.109578.

[2] Zhou Zhongyan, Liu Xiubo, Zhuang Suguo, et al. Preparation and high temperature tribological properties of laser in situ synthesized self-lubricating composite coatings containing metal sulfides on Ti6Al4V alloy[J]. Applied Surface Science, 2019, 481: 209–218. doi: 10.1016/j.apsusc.2019.03.092.

[3] Kümmel D, Schneider J, Gumbsch P. Influence of interstitial oxygen on the tribology of Ti6Al4V[J]. Tribology Letters, 2020, 68(3): 96. doi: 10.1007/s11249-020-01327-4.

[4] Cao Lei, Sun Hang, Wan Yong, et al. Tribological behavior of thermally oxidized TC4 titanium alloy under lubrication of a full formulated engine oil[J]. Tribology, 2019, 39(1): 17–25 (in Chinese) [曹磊, 孙航, 万勇, 等. 全合成机油润滑下热氧化改性TC4钛合金的摩擦学行为[J]. 摩擦学学报, 2019, 39(1): 17–25]. doi: 10.16078/j.tribology.2018122.

[5] Wang Junjun, Ma Jianjun, Huang Weijiu, et al. The investigation of the structures and tribological properties of F-DLC coatings deposited on Ti6Al4V alloys[J]. Surface and Coatings Technology, 2017, 316: 22–29. doi: 10.1016/j.surfcoat.2017.02.065.

[6] Manhabosco T M, Tamborim S M, dos Santos C B, et al. Tribological, electrochemical and tribo-electrochemical characterization of bare and nitrided Ti6Al4V in simulated body fluid solution[J]. Corrosion Science, 2011, 53(5): 1786–1793. doi: 10.1016/j.corsci.2011.01.057.

[7] Bewilogua K, Hofmann D. History of diamond-like carbon films-From first experiments to worldwide applications[J]. Surface and Coatings Technology, 2014, 242: 214–225. doi: 10.1016/j.surfcoat.2014.01.031.

[8] Kasiorowski T, Lin J, Soares P, et al. Microstructural and tribological characterization of DLC coatings deposited by plasma enhanced techniques on steel substrates[J]. Surface and Coatings Technology, 2020, 389: 125615. doi: 10.1016/j.surfcoat.2020.125615.

[9] Yan Mingming, Wang Xinyu, Zhang Songwei, et al. Friction and wear properties of GLC and DLC coatings under ionic liquid lubrication[J]. Tribology International, 2020, 143: 106067. doi: 10.1016/j.triboint.2019.106067.

[10] Han Xi, Zheng Jianyun, Zhang Shuaituo, et al. Microstructure and tribological properties of Al-DLC coatings in water[J]. Tribology, 2017, 37(3): 310–317 (in Chinese) [韩熙, 郑建云, 张帅拓, 等. Al-DLC薄膜结构及其在水介质下摩擦学性能研究[J]. 摩擦学学报, 2017, 37(3): 310–317]. doi: 10.16078/j.tribology.2017.03.005.

[11] Tanaka A, Suzuki M, Ohana T. Friction and wear of various DLC films in water and air environments[J]. Tribology Letters, 2004, 17(4): 917–924. doi: 10.1007/s11249-004-8100-2.

[12] Li An, Chen Qingchun, Wu Guizhi, et al. Probing the lubrication mechanism of multilayered Si-DLC coatings in water and air environments[J]. Diamond and Related Materials, 2020, 105: 107772. doi: 10.1016/j.diamond.2020.107772.

[13] Wu Xingyang, Chen Teng, Ge Zhou, et al. Tribological properties of N and Si Co-doped DLC films under different humidity conditions[J]. Tribology, 2017, 37(4): 501–509 (in Chinese) [吴行阳, 陈腾, 葛宙, 等. 不同湿度条件下N、Si共掺杂DLC膜的摩擦学性能研究[J]. 摩擦学学报, 2017, 37(4): 501–509]. doi: 10.16078/j.tribology.2017.04.012.

[14] Wang Xiongwei, Chai Liqiang, Pang Xianjuan, et al. Influence of salt spray test to DLC film on tribological properties[J]. Tribology, 2018, 38(4): 453–461 (in Chinese) [王雄伟, 柴利强, 逄显娟, 等. 盐雾腐蚀对DLC薄膜摩擦学性能的影响[J]. 摩擦学学报, 2018, 38(4): 453–461]. doi: 10.16078/j.tribology.2018.04.010.

[15] Waesche R, Hartelt M, Weihnacht V. Influence of counterbody material on wear of ta-C coatings under fretting conditions at elevated temperatures[J]. Wear, 2009, 267(12): 2208–2215. doi: 10.1016/j.wear.2009.08.041.

[16] Wang Fu, Lu Zhibin, Zhang Guangan, et al. Mating material-dependence of tribological behavior of fluorinated amorphous carbon-based films[J]. Tribology, 2017, 37(3): 357–363 (in Chinese) [王福, 鲁志斌, 张广安, 等. 氟化非晶碳基薄膜摩擦学行为对配副材料的依赖性[J]. 摩擦学学报, 2017, 37(3): 357–363]. doi: 10.16078/j.tribology.2017.03.011.

[17] Li H, Xu T, Wang C, et al. Tribochemical effects on the friction and wear behaviors of diamond-like carbon film under high relative humidity condition[J]. Tribology Letters, 2005, 19(3): 231–238. doi: 10.1007/s11249-005-6150-8.

[18] Zheng Shaoxian, Li Qiang, Huo Lei. Tribological mechanism analysis of DLC film and its different matings in CO_2 environment[J]. Journal of Lanzhou University of Technology, 2019, 45(5): 6–11 (in Chinese) [郑韶先, 李强, 霍磊. CO_2环境下DLC与不同对偶的摩擦学机理分析[J]. 兰州理工大学学报, 2019, 45(5): 6–11]. doi: 10.3969/j.issn.1673-5196.2019.05.002.

[19] Cui L, Lu Z, Wang L. Toward low friction in high vacuum for hydrogenated diamondlike carbon by tailoring sliding interface[J]. ACS Applied Materials & Interfaces, 2013, 5(13): 5889–5893. doi: 10.1021/am401192u.

[20] Wu Daheng, Ren Siming, Pu Jibin, et al. A comparative study of tribological characteristics of hydrogenated DLC film sliding against ceramic mating materials for helium applications[J]. Applied Surface Science, 2018, 441: 884–894. doi: 10.1016/j.apsusc.2018.01.206.

[21] Schwan J, Ulrich S, Batori V, et al. Raman spectroscopy on amorphous carbon films[J]. Journal of Applied Physics, 1996, 80(1): 440–447. doi: 10.1063/1.362745.

[22] Zhang S, Zeng X T, Xie H, et al. A phenomenological approach for the Id/Ig ratio and sp3 fraction of magnetron sputtered a-C films[J]. Surface and Coatings Technology, 2000, 123(2–3): 256–260. doi: 10.1016/S0257-8972(99)00523-X.

[23] Zhao Jiaqun, Li Liuhe, Jing Kai, et al. Effects of gradient interlayers on wear resistance of diamond-like coatings on cemented carbide[J]. Surface Technology, 2017, 46(1): 82–87 (in Chinese) [赵佳群, 李刘合, 景凯, 等. 梯度过渡层对硬质合金沉积类金刚石膜的耐磨性影响[J]. 表面技术, 2017, 46(1): 82–87]. doi: 10.16490/j.cnki.issn.1001-3660.2017.01.014.

[24] Wang Junjun, He Haoran, Huang Weijiu, et al. Effects of Cr-based interlayers on tribological property of diamond-like carbon films on titanium alloy[J]. China Surface Engineering, 2018, 31(3): 61–67 (in Chinese) [王军军, 何浩然, 黄伟九, 等. Cr基过渡层对钛合金表面类金刚石薄膜摩擦学性能的影响[J]. 中国表面工程, 2018, 31(3): 61–67]. doi: 10.11933/j.issn.1007-9289.20180108003.

[25] Lu Zhibin, wang Liping, Zhang Guangan, et al. The dependence of energy dissipation on the elastic energy density of friction pairs in hard coating films[J]. Tribology Letters, 2011, 41(2): 435–438. doi: 10.1007/s11249-010-9725-y.

[26] Bai Lichun, Zhang Guangan, Lu Zhibin, et al. Tribological mechanism of hydrogenated amorphous carbon film against pairs: a physical description[J]. Journal of Applied Physics, 2011, 110(3): 033521. doi: 10.1063/1.3619798.

[27] Shi Jing, Gong Zhenbin, Wang Yongfu, et al. Friction and wear of hydrogenated and hydrogen-free diamond-like carbon films: Relative humidity dependent character[J]. Applied Surface Science, 2017, 422: 147–154. doi: 10.1016/j.apsusc.2017.05.210.